Cancer Cell
Article

Targeting Mitotic Exit Leads to Tumor Regression In Vivo: Modulation by Cdk1, Mastl, and the PP2A/B55α,δ Phosphatase

Eusebio Manchado,[1] María Guillamot,[1] Guillermo de Cárcer,[1] Manuel Eguren,[1] Michelle Trickey,[2] Irene García-Higuera,[1,3] Sergio Moreno,[3] Hiroyuki Yamano,[2] Marta Cañamero,[4] and Marcos Malumbres[1,*]
[1]Cell Division and Cancer Group, Spanish National Cancer Research Centre (CNIO), E-28029 Madrid, Spain
[2]UCL Cancer Institute, University College London, London WC1E 6BT, UK
[3]Instituto de Biología Molecular y Celular del Cáncer, CSIC/Universidad de Salamanca, E-27007 Salamanca, Spain
[4]Comparative Pathology Unit, CNIO, E-28029 Madrid, Spain
*Correspondence: malumbres@cnio.es
DOI 10.1016/j.ccr.2010.10.028

SUMMARY

Targeting mitotic exit has been recently proposed as a relevant therapeutic approach against cancer. By using genetically engineered mice, we show that the APC/C cofactor Cdc20 is essential for anaphase onset in vivo in embryonic or adult cells, including progenitor/stem cells. Ablation of Cdc20 results in efficient regression of aggressive tumors, whereas current mitotic drugs display limited effects. Yet, Cdc20 null cells can exit from mitosis upon inactivation of Cdk1 and the kinase Mastl (Greatwall). This mitotic exit depends on the activity of PP2A phosphatase complexes containing B55α or B55δ regulatory subunits. These data illustrate the relevance of critical players of mitotic exit in mammals and their implications in the balance between cell death and mitotic exit in tumor cells.

INTRODUCTION

Multiple efforts in the last two decades have been put toward the evaluation of therapeutic advantages of cell cycle inhibition in tumor cells (Malumbres and Barbacid, 2009). These strategies include impairing the entry into the cell cycle by inhibition of cyclin-dependent kinases (Cdks), arresting cells at the G1/S or G2/M transitions with DNA-damaging agents, or inhibiting mitotic progression by targeting microtubules or mitotic kinases (Jackson and Bartek, 2009; Jordan and Wilson, 2004; Malumbres and Barbacid, 2001, 2007). In most cases, tumor proliferation is only transiently or partially reduced. For instance, inhibiting G1 Cdks only results in minor defects given the compensation between multiple family members, and G0/G1-arrested cells can resume cell cycle proliferation upon activation of the appropriate stimuli (Malumbres and Barbacid, 2009). Checkpoint-mediated arrest can be transient once the insulting conditions have been eliminated or repaired or as a result of adaptation to the checkpoints (Syljuasen, 2007; Weaver and Cleveland, 2005). In addition, resistance to microtubule poisons can be acquired by expression of particular tubulin isoforms or microtubule-regulating proteins (Kavallaris, 2010), and cells can display many variable fates following exposure to microtubule drugs (Gascoigne and Taylor, 2008).

More recently, mitotic exit has been proposed as a relevant target given the proapoptotic effect of RNA interference (RNAi) against the anaphase-promoting complex/cyclosome (APC/C) cofactor Cdc20 (Huang et al., 2009). Chromosome segregation requires the activity of the APC/C, an E3 ubiquitin ligase that targets critical cell cycle regulators for degradation (Peters, 2006; Sullivan and Morgan, 2007). APC/C recognizes its substrates through two adaptor proteins, Cdc20 and Cdh1. Cdc20 is responsible for APC/C function during the early phases of mitosis and for triggering mitotic exit at the metaphase-to-anaphase transition. Cdh1 activates the APC/C during the final phases of mitosis and G1 (Peters, 2006). The current model states that, upon complete bipolar attachment of all chromosomes to spindle microtubules, the activation of APC/C by Cdc20 results in the elimination of two critical targets: securin, a separase inhibitor; and cyclin B, the activating subunit of

Significance

Despite the multiple efforts to inhibit the cell cycle in tumors, most therapeutic approaches are limited due to compensatory effects or by adaptation to the therapeutic conditions. We show in this manuscript that mammalian cells require Cdc20 for anaphase onset in vivo. Genetic ablation of Cdc20 results in dramatic tumor regression due to apoptotic cell death, whereas parallel treatments with current mitotic drugs display more limited effects. Inhibition of the kinases Cdk1 and Mastl mediates a PP2A-B55-dependent mitotic exit and protection from apoptosis in Cdc20-depleted cells. Full understanding of this pathway is likely to be critical for improving strategies aimed to target mitotic exit for cancer treatment.

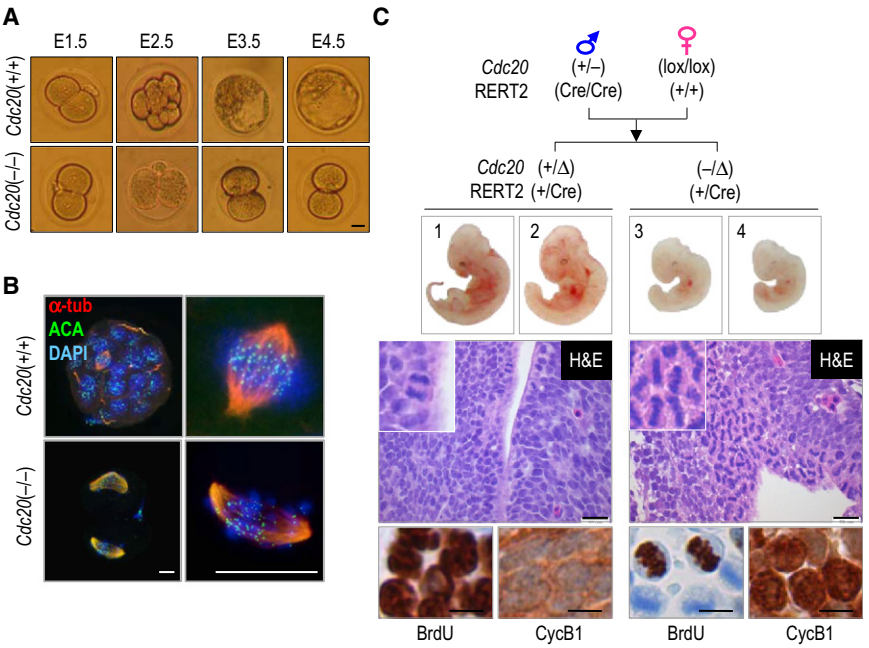

Figure 1. Cdc20 Is Essential for Anaphase Onset in Embryonic Cells

(A) Cdc20 null embryos (Figure S1) arrest at the two-cell stage, whereas wild-type embryos progress to blastocysts by embryonic (E) days 3.5–4.5. Scale bars, 20 μM.

(B) Immunofluorescence analysis of E3.5 embryos showing normal mitotic figures in *Cdc20*(+/+) morulas. *Cdc20*(–/–) embryos arrest at the two-cell stage and display condensed chromosomes without separation of sister chromatids. α-tubulin, red; Anti-centromeric antigen, ACA, green; DAPI, blue. Scale bars, 10 μM.

(C) *Cdc20*(lox/lox); RERT2(+/+) females were crossed with *Cdc20*(+/–); RERT2(Cre/Cre) males, injected with 4-OHT by E10.5 or E12.5 (Figure S2), and embryos were extracted 24 hr later. In control (*Cdc20*(+/Δ); RERT2(+/Cre)) samples, most cells are interphasic or display anaphase figures (insets), as observed in the proliferating neuroepithelium. Cdc20-deficient embryos display a dramatic accumulation of cells in metaphase. Some of these metaphases are positive for BrdU after a 6 hr pulse with this marker. However, most metaphase cells are negative for BrdU, indicating that they have been arrested in metaphase during longer periods. Cdc20 null cells also display a dramatic accumulation of cyclin B1 after specific immunostaining. Scale bars, 20 μM (H&E) or 10 μM (immunohistochemistry).

Cdk1. This results in the subsequent inhibition of Cdk1 and activation of separase, a protease that cleaves cohesion complexes that maintain sister chromatids together (Peters, 2006; Sullivan and Morgan, 2007). In yeast, inhibition of Cdk1 and separase activity also results in the activation of Cdc14 phosphatases that remove mitotic phosphates, thus triggering mitotic exit (Stegmeier and Amon, 2004; Sullivan and Morgan, 2007). The overall mechanism is thought to be conserved in vertebrates, although the relevance of the different molecular pathways involved is not clear. First, strong RNAi against Cdc20 or the APC/C catalytic subunit Apc2 has failed to induce mitotic arrest in some studies (Baumgarten et al., 2009; Gimenez-Abian et al., 2005), probably as a consequence of residual Cdc20 activity (Wolthuis et al., 2008). Second, inhibition of Cdk1-cyclin B may be insufficient for mitotic exit in the presence of proteasome inhibitors, and a new mechanism involving proteasome-dependent degradation of phosphatase inhibitors has been proposed (Skoufias et al., 2007). Finally, vertebrate Cdc14 phosphatases do not seem to play a critical role in mitotic exit (Queralt and Uhlmann, 2008), and PP1 or PP2A may function as mitotic exit phosphatases, at least in *Xenopus* (Mochida et al., 2009; Vigneron et al., 2009; Wu et al., 2009). In this manuscript we investigate the requirements for mitotic exit in mammals and their implication in cancer therapy by using a conditional mutation in the murine *Cdc20* gene.

RESULTS

Genetic Ablation of Cdc20 Results in Metaphase Arrest In Vivo

The conditional null mutation in the mouse *Cdc20* gene was generated by homologous recombination in ES cells (see Figure S1 available online). *Cdc20*(+/–) mice are viable and fertile. As previously shown using a gene-trap allele (Li et al., 2007), lack of Cdc20 results in embryonic lethality at the two-cell stage (Figures 1A and 1B). These cells arrest in metaphase by E1.5 and display abnormal mitotic figures during the following days, probably as a consequence of prolonged metaphase arrest. For conditional ablation in vivo, we made use of a conditional allele (*Cdc20*(lox)) in which exon 2 is flanked by loxP sites (Figure S1). In these animals a tamoxifen-inducible form of the Cre recombinase (Cre-ERT2) (Guerra et al., 2003) is expressed from the 3′-UTR of the RNA polymerase II gene (RERT allele). Pregnant females were treated at E10.5 (Figure 1C) or E12.5 (Figure S2) with 4-hydroxytamoxifen (4-OHT) to induce Cre activity and excision of exon 2 (*Cdc20*(Δ) allele). *Cdc20*(–/Δ); RERT(+/Cre) embryos that inherit a *Cdc20*(–) null allele and a *Cdc20*(lox) allele display a dramatic arrest in development 24 hr after activation of the Cre recombinase with 4-OHT. A detailed histological analysis of these samples reveals a general proliferative arrest characterized by the presence of abundant metaphase figures and high levels of cyclin B in all proliferating tissues (Figure 1C; Figure S2).

To further investigate whether Cdc20 is also required at post-embryonic stages, we fed 1 month old *Cdc20*(–/lox); RERT (+/Cre) mice and control littermates carrying a *Cdc20*(+) wild-type allele or lacking Cre with a 4-OHT supplemented diet. This treatment does not significantly modify the viability of control mice. However, all *Cdc20*(–/Δ); RERT(+/Cre) mice die after 8–10 days on the 4-OHT diet (Figure 2A). This death is likely to be associated with the dramatic loss of weight in *Cdc20*(–/Δ); RERT(+/Cre) mice, but not in the *Cdc20*(+/Δ); RERT(+/Cre), *Cdc20*(+/lox); RERT(+/+), or *Cdc20*(–/lox); RERT(+/+) control groups (Figure 2B). Genetic disruption of Cdc20 results in several histological abnormalities in different tissues. Specifically,

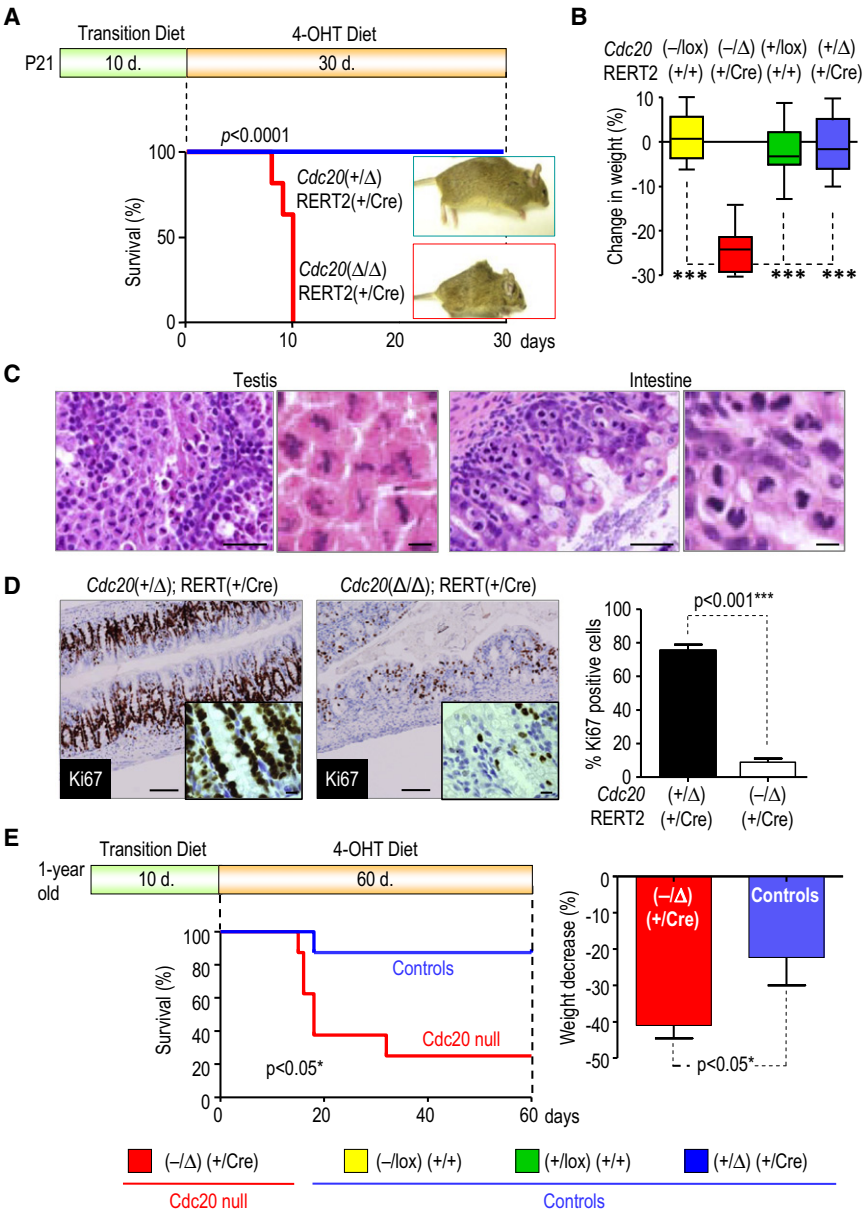

Figure 2. Cdc20 Is Essential for Proliferation in Adult Mice

(A and B) Young mice (P21) were fed with a transition diet and then supplemented with 4-OHT (A). This results in rapid lethality in *Cdc20*(−/Δ); RERT2(+/Cre) mice that correlates with (B) a dramatic loss of weight. ***p < 0.0001.

(C) These Cdc20-deficient mice display abundant metaphase-arrested cells in most proliferating tissues, including the testis and the intestine. H&E staining.

(D) Cell proliferation (Ki67) in the intestine of young *Cdc20*(−/Δ);RERT(+/Cre) and control *Cdc20*(+/Δ); RERT(+/Cre) mice after conditional induction of Cre. The ratio of Ki67-positive cells in the epithelium is also plotted. Similar differences are found in testis and spleen (Figure S2).

(E) Conditional ablation of Cdc20 in 1 year old mice. These animals were exposed to a transition diet for 10 days and then supplemented with 4-OHT for 60 days. Control animals (blue) included *Cdc20*(+/lox);RERT(+/+) (n = 4), *Cdc20*(−/lox); RERT(+/+) (n = 4), and *Cdc20*(+/Δ);RERT(+/Cre) (n = 4). Mice with these genotypes displayed a similar behavior and are grouped in the analysis. Cdc20 null mice (*Cdc20*(−/Δ);RERT(+/Cre); n = 8; green) displayed a significant reduction in weight, and most of them died within the first month. However, two of these Cdc20 mutant mice survived during the assay, similarly to control mice. Scale bars, 50 or 10 μM (insets).

Data in (B), (D), and (E) are represented as mean ± SD.

proliferative areas in diverse tissues such as intestine and testis display abundant mitotic figures representative of metaphases, suggesting that the lack of Cdc20 causes widespread metaphase arrest in proliferating cells in vivo (Figures 2C and 2D; Figure S2). The phenotype induced by Cdc20 loss in intestinal epithelium suggests that *Cdc20*(−/Δ); RERT(+/Cre) mice die because of impaired absorption of nutrients. Genetic ablation of Cdc20 in older (1 year old) mice results in similar cellular defects in proliferating cells. However, these treated mice display improved survival. Two out of eight older mice can survive for several months despite the absence of Cdc20 expression, suggesting that these mice are less susceptible to the physiological consequences of loss of proliferation (Figure 2E).

Cdc20 Is Essential for Anaphase Onset in Progenitor and Tumor Cells

To determine whether genetic ablation of Cdc20 is less harmful in quiescent cells, we analyzed slowly proliferating progenitor/stem cells. A single topical treatment with 4-OHT in *Cdc20*(−/lox); RERT(+/Cre) mice results in a significant increase in metaphase figures in the basal layer of the epidermis. However, no metaphase figures are observed in the hair follicles, where hair progenitor/stem cells reside (Figure 3A). To induce proliferation of progenitor cells and hair regeneration, mice were depilated 8 days after a single 4-OHT application. Following this treatment, abundant metaphase figures are observed in multiple cells in the hair follicles, including CD34-positive progenitor cells. This hair regeneration response is impaired in *Cdc20*(−/Δ); RERT(+/Cre) mice without the need of further 4-OHT applications (Figure 3A). These data suggest that elimination of Cdc20 in nonproliferating cells is silent during quiescence or interphase; however, metaphase arrest is observed once these cells are committed to cell division. Similar ablation of Cdc20 in hematopoietic progenitor/stem cells also results in metaphase arrest and complete impairment in the formation of colonies ex vivo (Figures 3B and 3C).

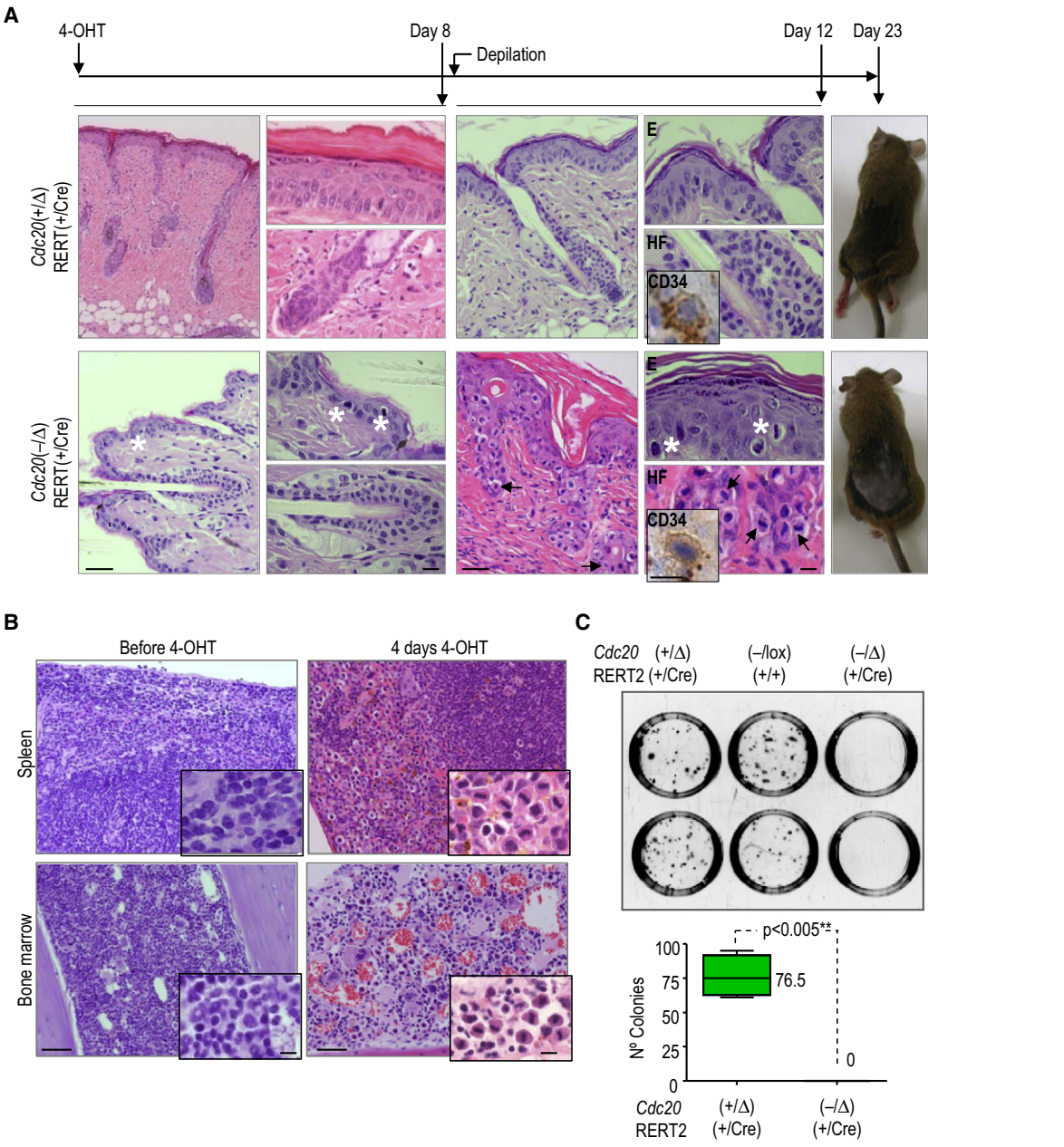

Figure 3. Cdc20 Is Essential for Mitosis in Progenitor Cells

(A) Eight days after a single topical treatment with 4-OHT, a significant number of proliferating cells in the basal layer of the epidermis (E) are arrested in mitosis (asterisks) in Cdc20-deficient (*Cdc20*(−/Δ); RERT2(+/Cre)), but not control (*Cdc20*(+/Δ); RERT2(+/Cre)) mice. No metaphase figures are observed in the hair follicles (HF). After depilation of these animals, most hair follicles are abnormal and display abundant cells arrested in mitosis (arrows) without further treatment with 4-OHT. Some of these metaphase cells are positive for CD34, a marker of hair follicle progenitors. This does not represent normal mitotic proliferation because hair regeneration is significantly impaired in these Cdc20-deficient mice, as observed in the back of these animals 15 days after depilation. H&E staining or immunodetection of CD34 (insets). Bars indicate 50 or 10 μm (CD34 insets).

(B) Representative micrographs of *Cdc20*(−/Δ);RERT(+/Cre) spleen and bone marrow before and after treatment with 4-OHT. Metaphase figures are abundant 4 days after treatment with 4-OHT in both organs. H&E staining. Scale bars, 50 or 10 μM (insets).

(C) Colony formation assay of hematopoietic precursors. Equal number of cells from the bone marrow of the indicated genotypes was plated in Methocult plates. These cells were then cultured in the presence of 4-OHT, and the number of colonies (mean ± SD) was scored after 12 days.

The strong requirement for Cdc20 in normal proliferative cells prompted us to analyze whether Cdc20 is also essential for mitosis in tumor cells in vivo. Skin tumors were induced using the two-stage carcinogenesis protocol in *Cdc20*(−/lox) mice expressing the inducible Cre recombinase. 4-OHT was topically applied on the skin when these tumors reached a volume of 50 mm^3 (about 4 weeks after they were first observed). As shown in Figures 4A and 4B (and Figure S3), tumors continue to grow

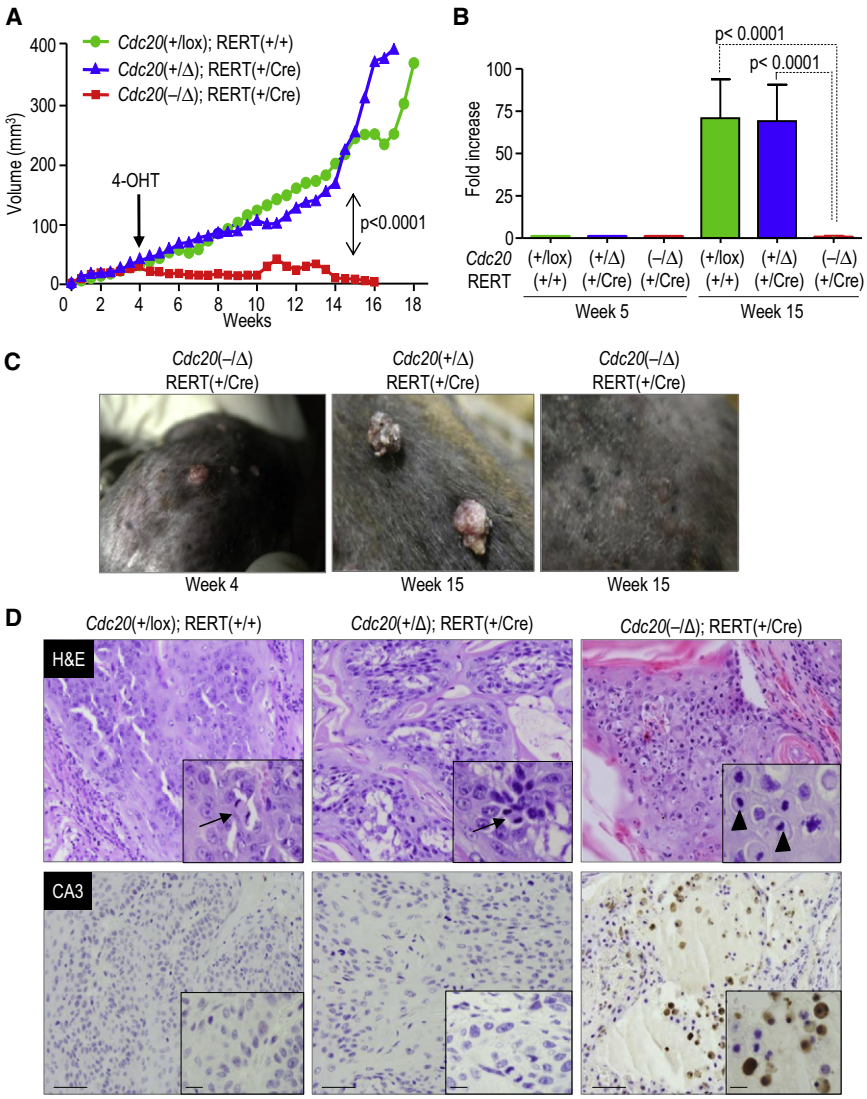

Figure 4. Cdc20 Ablation Results in Arrest of Skin Tumors In Vivo

(A) Skin tumors were induced by the two-stage carcinogenesis protocol, and papillomas were topically treated with 4-OHT when they reached 50 mm^3 of volume.

(B) Fold increase in tumor volume by week 5 (1 week after treatment with 4-OHT) or week 15 (mean ± SD). See also Figure S3.

(C) Representative pictures of papillomas before (week 0) or after treatment (week 15).

(D) Micrographs of skin tumor sections (week 15) of the indicated genotypes showing a few mitotic figures (anaphase; arrows) in control tumors and massive mitotic arrest (mostly metaphase; arrowheads) and apoptosis (active-caspase 3 (CA3)-positive cells) in Cdc20-deficient tumors. Scale bars, 50 or 10 μM (insets).

exponentially in *Cdc20*(+/lox); RERT(+/+) as well as *Cdc20*(+/Δ); RERT(+/Cre) mice. However, these tumors arrest completely in *Cdc20*(−/Δ); RERT(+/Cre) mice soon after 4-OHT treatment. In most cases these tumors acquire a whitish appearance, dry, and fall off and are no longer observed in the skin of these treated mice (Figure 4C). Histological observation of treated tumor samples indicates that lack of Cdc20 results in a massive arrest of tumor cells in metaphase-like stages. These tumor samples also contain abundant apoptotic figures (Figure 4D) that are not frequently observed in normal Cdc20-deficient epithelial tissues.

Since these skin tumors are relatively benign, we also analyzed aggressive fibrosarcomas induced by *Cdc20*(lox/lox); RERT(+/Cre) fibroblasts expressing H-ras V12 and E1A, two oncogenes that disrupt major tumor suppressor pathways, such as the retinoblastoma protein route in human tumors. Primary mouse embryonic fibroblasts (MEFs) were transfected with RasV12 and E1A-expressing vectors, and transformed foci were used to generate stable clones. Application of 1 μM 4-OHT in these cultures results in a dramatic mitotic arrest at 24 hr, and most cells are either arrested in metaphase or apoptotic at 48 hr (Figures 5A–5D). The application of 4-OHT has no effect in *Cdc20*(+/lox); RERT(+/Cre) control cells (data not shown). When *Cdc20*(lox/lox); RERT(+/Cre) or control transformed cells are injected in SCID-immunosuppressed mice, rapid and aggressive fibrosarcomas are observed within 1–2 weeks. 4-OHT was systemically applied to these animals when tumors reached ∼350 mm^3, and tumor volume was scored afterward. As displayed in Figures 5E and 5F, and Figure S3, the size of all these tumors slightly increased during the first 1–3 days after 4-OHT treatment. However, *Cdc20*(Δ/Δ); RERT(+/Cre) tumors stop growing and dramatically regress until they are almost undetectable 16 days after treatment. Control tumors, on the other hand, grow exponentially until mice were sacrificed for ethical reasons. Histological examination of *Cdc20*(lox/lox); RERT(+/Cre) untreated tumors or control (*Cdc20*(lox/lox); RERT(+/+) or Cdc20(+/+); RERT(+/Cre)) tumors treated with 4-OHT during 8 days shows frequent mitotic (mostly anaphase) figures in agreement with the rapid growth of these tumors. However, *Cdc20*(Δ/Δ); RERT(+/Cre) tumors treated with 4-OHT display massive mitotic arrest and apoptotic cell death (as measured by active caspase 3) as soon as 4 days after treatment (Figure 5G). We have also tested whether apoptotic cell death in Cdc20-deficient cells is mediated by p53 by using *Cdc20*(lox/lox); *p53*(−/−) double-mutant MEFs. In these cells the apoptotic cell death induced by Cdc20 ablation is not prevented by p53 deletion (Figure S3). Overall, these results indicate that Cdc20-directed therapies may be efficient in most tumor types, regardless of their alteration in Ras, pRb, or p53 routes, three of the most frequently mutated pathways in human cancer.

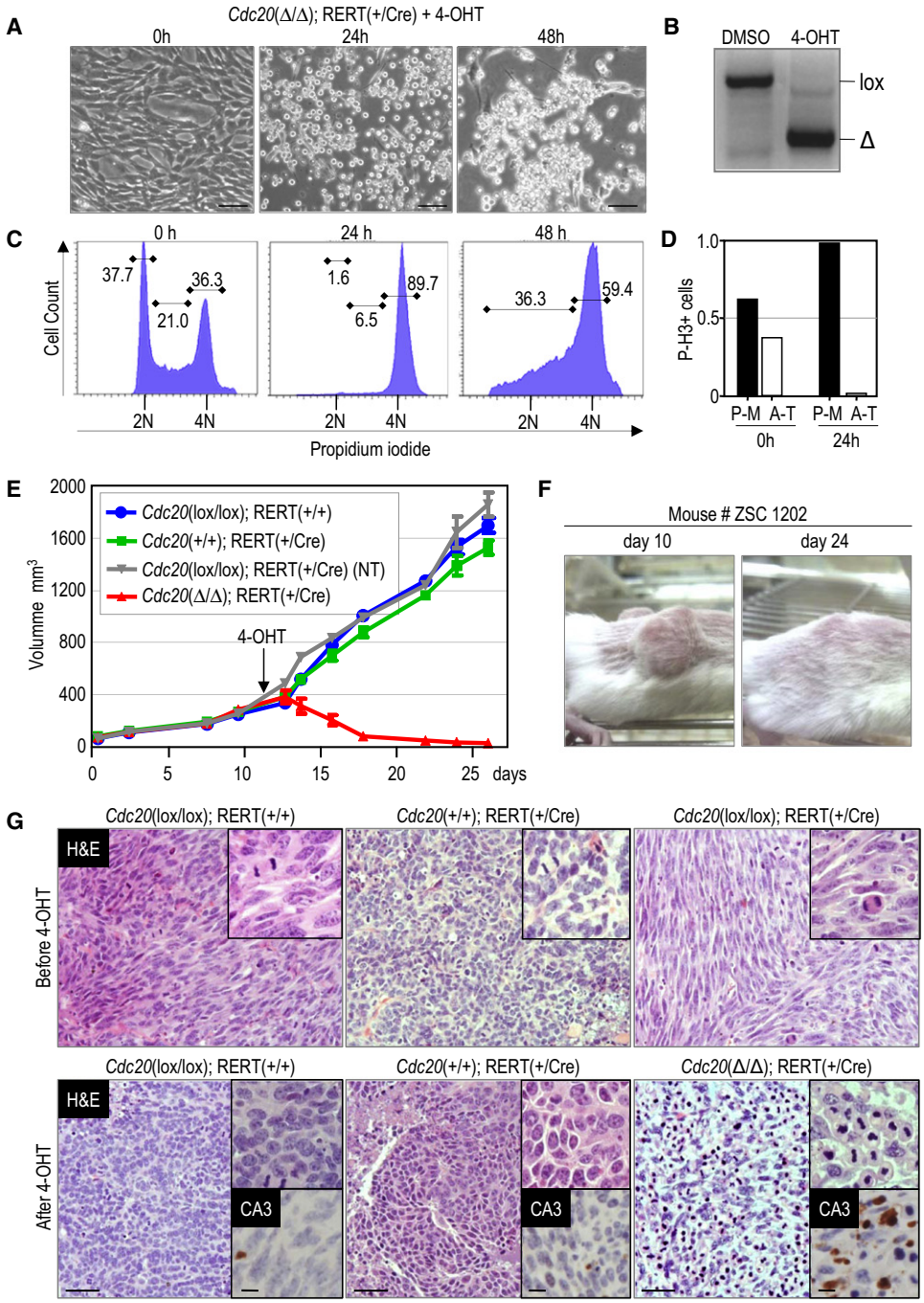

Figure 5. Elimination of Cdc20 Results in Complete Regression of Aggressive Tumors In Vivo

(A) *Cdc20*(lox/lox); RERT(+/Cre) MEFs were transformed with a combination of Ras + E1A oncogenes, and *Cdc20* exons were excised adding 1 μM 4-OHT. Scale bars, 50 μM.

(B) Efficient excision of Cdc20 exons generating the *Cdc20*(Δ) allele 48 hr after addition of 4-OHT.

(C) Propidium iodide staining showing a dramatic accumulation of 4N *Cdc20*(Δ/Δ); RERT(+/Cre) cells 24 hr after addition of 4-OHT. Most sub-4N cells at 48 hr correspond to apoptotic cells as determined by Annexin V staining (Figure S4).

(D) Detection of phospho-histone H3 (P-H3) cells by immunofluorescence 0 and 24 hr after addition of 4-OHT. P-M, prophase to metaphase; A-T, anaphase and telophase.

(E) Ras+E1A transformed MEFs of the indicated genotypes were subcutaneously injected in SCID mice, and tumors were scored every 3 days. These mice were then injected i.p. (three injections in 1 week) with 4-OHT when the aggressive subcutaneous tumors reached about 350 mm^3 of volume (day 12; arrow). Ten tumors of each genotype treated with 4-OHT or non-treated (NT) were scored. The average tumor volume ± SEM is shown. See Figure S3 for additional data.

(F) Representative images of a fibrosarcoma in a *Cdc20*(lox/lox); RERT(+/Cre) mouse before (day 10) and 14 days (day 24) after 4-OHT.

Efficient Mitotic Arrest and Apoptosis in the Absence of Cdc20

Multiple mitotic drugs are currently used in the clinic to treat tumors, and new small-molecule inhibitors are under clinical development. Therefore, we compared the effects of Cdc20 ablation with microtubule stabilizing (taxol) or destabilizing (vincristine) agents or with two mitotic drugs currently in clinical trials: BI2536 (a Plk1 inhibitor) and monastrol (an inhibitor of the kinesin Eg5). Tumoral *Cdc20*(lox/lox); RERT(+/Cre); H-ras-E1A cells co-expressing a histone H2B-GFP reporter were treated with 4-OHT (to disrupt Cdc20) or with the indicated drugs, and their fate was followed by videomicroscopy during 3 days. Control cells (treated with DMSO) typically undergo 3–4 cell divisions, whereas genetic ablation of Cdc20 results in metaphase arrest. All Cdc20-deficient cells undergo apoptosis from this mitotic arrest with an average latency of 20 ± 11 hr, as detected by videomicroscopy and Annexin-V staining (Figure 6A; Figure S4). Interestingly, this dramatic effect is not achieved by any of the administrated mitotic drugs. Whereas a few cells die in mitosis or interphase (red and green lines in Figure 6A), most cells treated with these chemicals are alive and undergo several rounds of mitotic entry and exit. In fact, whereas Cdc20 ablation kills 50% of cells by 18 hr after mitotic entry, none of the drugs reaches these levels of lethality during the 72 hr recorded in this assay (Figures 6A and 6B). In addition, about 50% of cells treated with mitotic drugs incorporate the nucleotide analog EdU when added 24 hr after the mitotic inhibitors. This figure is reduced to less than 10% in *Cdc20*(lox/lox); RERT(+/Cre) cells after 4-OHT treatment (Figure S4). This background is probably due to cells in which 4-OHT was not active or in which the remaining amount of Cdc20 was enough for mitotic exit. In fact all these cells arrest in metaphase in the following cycle as observed by videomicroscopy (data not shown). DNA replication in cells treated with mitotic drugs results in increased ploidy that is not observed in Cdc20 null cells (Figure S4).

Given the relevance of mitotic poisons in the clinic, we also compared the therapeutic effect of Cdc20 ablation versus standard treatments with taxol, vincristine, or the Plk1 inhibitor BI2536. *Cdc20*(lox/lox); RERT(+/Cre); H-ras; E1A cells were injected into SCID mice as described above, and 4-OHT or the indicated drugs were injected i.p. 11 days after the xenotransplant (tumor size ~200 mm^3). These treatments were repeated three times a week. In these conditions, control tumors grow exponentially, whereas genetic ablation of Cdc20 results in complete tumor regression in about 10 days. In comparison, treatment with taxol, vincristine, and BI2536 only induces partial responses (Figure 6C). In agreement with the data observed in vitro, immunohistochemical analysis of samples taken 3 days after the first treatment indicates lack of proliferation (as measured by BrdU incorporation) and massive apoptosis in Cdc20 null cells, whereas all other samples maintain significant levels of proliferation and reduced apoptotic markers (Figure 6D; Figure S4).

Inactivation of Mastl Synergizes with Cdk1 Inhibition in Mitotic Exit Downstream of Cdc20

To gain further insights into the molecular defects caused by lack of Cdc20, primary *Cdc20*(lox/lox) MEFs were transduced with adenoviruses expressing either the green fluorescent protein (GFP) or the Cre recombinase. Expression of Cre, but not GFP, in confluent cells efficiently excises exon 2 resulting in the *Cdc20*(Δ) null allele, and results in the accumulation of mitotic (MPM2-positive and phospho-H3-positive) cells (Figure S5). These *Cdc20*(Δ/Δ) cells are arrested in metaphase, whereas post-metaphase figures (anaphase, telophase, or cytokinesis) are rarely observed. Lack of Cdc20 results in a significant increase in cyclin B1 and cyclin A2 protein levels, whereas the stabilization of securin is not as evident. Mad2 and $p21^{Cip1}$ protein levels are decreased in Cdc20 null cells, suggesting that the spindle assembly checkpoint is satisfied and that $p21^{Cip1}$ may be targeted by additional proteolytic regulators (Figure S5).

We next tested whether the elimination of securin and cyclin B could rescue the metaphase arrest in Cdc20 null cells as previously demonstrated in yeast (Shirayama et al., 1999; Thornton and Toczyski, 2003; Wäsch and Cross, 2002). Individual knockdown of securin or cyclin B1 by RNAi did not rescue the mitotic arrest of Cdc20 null cells (data not shown). Because mammalian cells also express other B-type cyclins that can compensate for lack of cyclin B1, we decided to test the effect of chemical inhibitors of Cdks. Cdc20-depleted cells were treated with small-molecule inhibitors of Cdks (roscovitine, purvalanol A, RO-3306, and GCP-74514A) or other kinases such as Plk1 (GW843682X) or Aurora B (ZM447439) as additional controls. In addition a general kinase inhibitor (staurosporine) with preference to AGC (PKC family) kinases was also used. Mitotic exit (as determined by loss of rounded, morphology, decondensation of chromosomes, and loss of phospho-MPM2, phospho-H3, and Cdk-dependent phosphosites) is induced by the Cdk inhibitors RO-3306 and GCP-74514A whereas two other Cdk inhibitors (roscovitine and purvalanol A) are not efficient in inducing mitotic exit in this assay (Figure S5). These differences have been previously observed in human cells treated with proteasome inhibitors (Potapova et al., 2006; Skoufias et al., 2007), and they are likely to be due to differences in specificity and potency of these drugs.

To further study the components of the mitotic exit machinery in Cdc20 null cells, we decided to use roscovitine for three reasons. First, it is a very specific inhibitor of Cdks (Bain et al., 2007). Second, it significantly inhibits Cdk1 kinase activity, even in Cdc20 null cells that display strong Cdk1 activity (Figure S5). Finally, it rapidly induces mitotic exit in nocodazole-arrested cells (Figures 7A and 7B), in agreement with the requirements for Cdk1 activity to sustain the spindle assembly checkpoint in these conditions (D'Angiolella et al., 2003). In Cdc20 null cells, neither roscovitine alone nor the combination of roscovitine and securin RNAi allows sister chromatid separation or mitotic exit, and these cells remain in metaphase

(G) Histological sections of tumors 4 days after the first injection with 4-OHT (day 16). Upper insets represent anaphase figures surrounded by interphase figures in control tumors or before the application of 4-OHT. *Cdc20*(Δ/Δ); RERT(+/Cre) tumors massively arrest in metaphase 4 days after treatment and accumulate frequent apoptotic figures (lower insets). CA3, immunodetection of active caspase 3. Scale bars, 50 or 10 μM (insets).

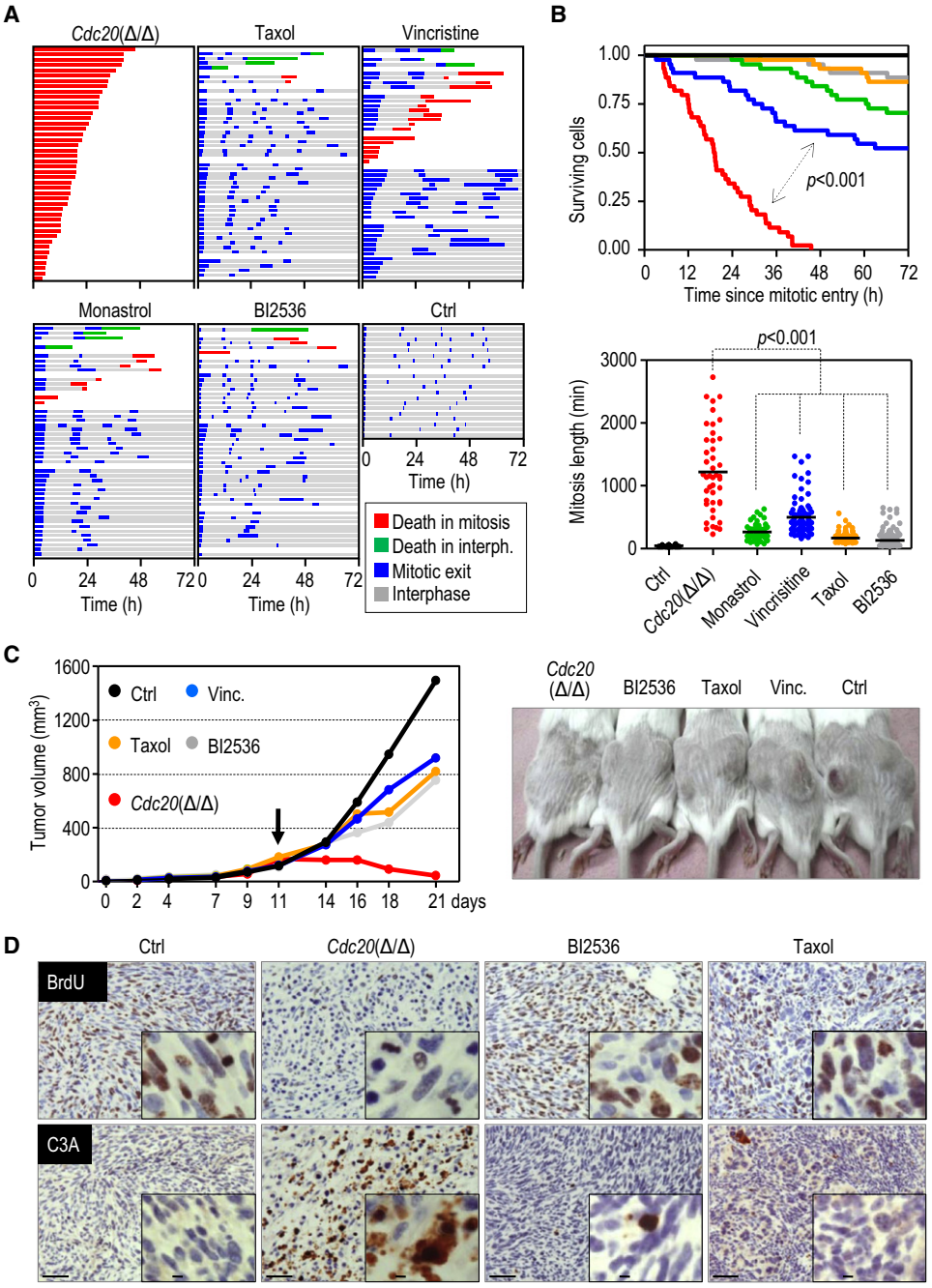

Figure 6. A Comparison between Genetic Ablation of Cdc20 and Current Mitotic Drugs

(A) *Cdc20*(lox/lox); RERT(+/Cre); H2B-GFP cells transformed with H-ras and E1A oncogenes were treated with 4-OHT to generate *Cdc20*(Δ/Δ) cells or with the indicated mitotic inhibitors. Twenty-four hours after the treatment, cells were recorded by videomicroscopy during an additional 72 hr, and their transition trough mitosis or interphase is shown by colored lines. Red or green lines indicate mitosis or interphase ending in apoptosis. Blue and gray lines indicate normal alternation between mitosis and interphase. Every raw indicates the fate of individual cells (n = 44 per treatment).

(B) Ratio of live cells and duration of mitosis in Cdc20 null cells (red) and control *Cdc20*(lox/lox) cells treated with vincristine (blue), monastrol (green), taxol (orange), and the Plk1 inhibitor BI2536 (gray). All Cdc20 null cells die within 48 hr without being able to exit mitosis, whereas more than half of the cells treated with mitotic drugs exit mitosis and are viable during the first 72 hr.

(C) Transformed *Cdc20*(lox/lox); RERT(+/Cre) MEFs were subcutaneously injected into the two flanks of SCID mice, and tumors were scored every 2–3 days. These mice were injected i.p. (three injections per week) with 4-OHT or mitotic drugs (taxol, vincristine, and BI2536) when tumors reached about 200 mm^3 of volume (day 11; arrow) (n = 8 mice per group).

(D) Representative images of these fibrosarcomas 3 days after injection with 4-OHT (to generate *Cdc20*(Δ/Δ) cells), BI2536, or taxol. These mice were injected with 10 μM BrdU to score DNA replication. CA3, immunodetection of active caspase 3. Scale bars, 50 or 10 μM (insets). Additional data are shown in Figure S4.

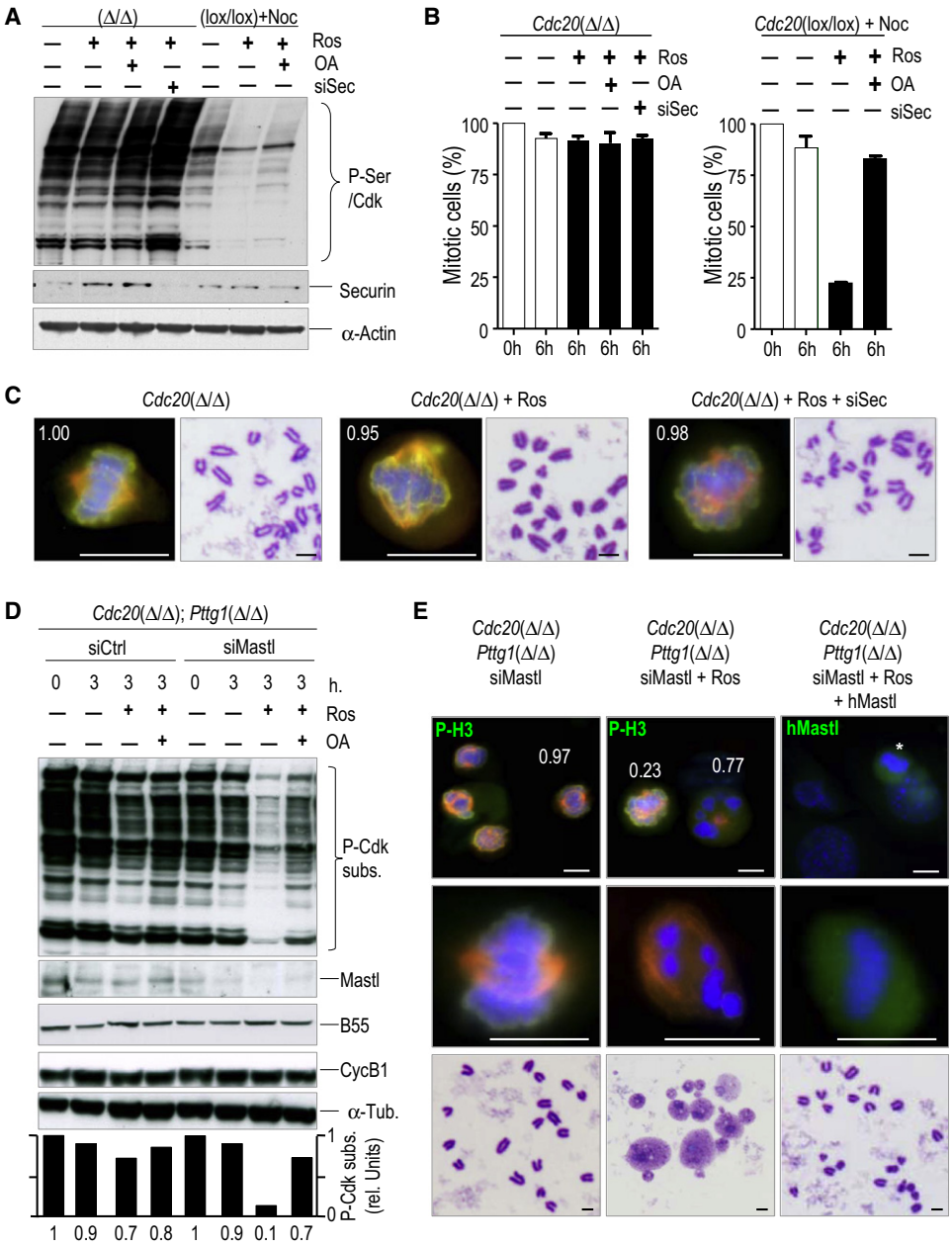

Figure 7. Cdc20-Dependent Mitotic Exit Can Be Triggered by Concomitant Inhibition of Cdk and Mastl Kinases

(A) *Cdc20*(lox/lox) cells were infected with AdCre (*Cdc20*(Δ/Δ)) or treated with nocodazole (Noc), siRNAs against securin (siSec), roscovitine (Ros), or okadaic acid (OA). None of these treatments induced mitotic exit (as measured by dephosphorylation of Cdk substrates) in Cdc20-deficient cells, although Ros induced an OA-inhibitable mitotic exit in nocodazole-arrested cells (see also Figure S5).

(B) The percentage of mitotic cells (mean ± SD as scored by DAPI staining) in the different conditions is indicated in the histograms showing strong correlation with the Cdk-dependent phospho-Ser mark.

(C) Representative metaphase-arrested cells in the previous assay. The ratio of metaphase cells is indicated (normalized to *Cdc20*(Δ/Δ)). Phospho-histone H3, yellow; α-tubulin, red; DAPI, blue. Metaphase spreads are shown in the right panels indicating cohesion between sister chromatids in these cells.

(D) Double-mutant *Cdc20*(Δ/Δ); *Pttg1*(Δ/Δ) cells were transfected with siRNAs against Mastl (siMastl) or scrambled siRNAs (siCtrl). These cells were also treated with roscovitine (Ros) or OA as indicated and analyzed 48 hr postinfection with AdCre (0 hr) or after 3 hr in the presence of Ros and/or OA. Mitotic exit is only observed after concomitant inhibition of Cdk1 and elimination of Mastl. The indicated proteins or phospho-epitopes were analyzed by immunoblotting, and the relative levels of phospho-Cdk-substrates are normalized versus siCtrl at t = 0.

(E) Representative micrographs of cells or metaphase spreads in these cultures. The ratio of cells in metaphase or with decondensed chromosomes is indicated (normalized to cells treated with scramble siRNAs). An additional culture (right panels) shows the effect of a human GFP-tagged-Mastl cDNA insensitive to siRNAs (hMastl; green signal). P-H3, yellow; α-tubulin, red; DAPI, blue. Scale bars indicate 10 μM in immunofluorescence images and 2 μM in metaphase spreads.

without separation of sister chromatids (Figures 7A–7C; Figure S5). We also combined *Cdc20* mutant alleles with *Pttg1* (encoding securin) conditional alleles (Wirth et al., 2006), thus eliminating any residual securin after RNAi assays. *Cdc20*(Δ/Δ); *Pttg1*(Δ/Δ) double-mutant MEFs arrest in metaphase similarly to *Cdc20*(Δ/Δ); *Pttg1*(+/+) cells, and the addition of roscovitine has only a minor effect on mitotic exit (Figure 7D; Figure S5). Roscovitine-treated Cdc20; securin null cells are arrested in metaphase with high levels of phosphorylation of Cdk substrates (Figures 7D and 7E), suggesting that mitotic phosphatases cannot be activated in the absence of Cdc20. The fact that 500 nM of okadaic acid (OA), a concentration known to preferentially inhibit PP2A (Felix et al., 1990; Wu et al., 2009), prevents mitotic exit by roscovitine in nocodazole-arrested cells (Figures 7A and 7B) (Skoufias et al., 2007), suggests that PP2A may participate in mammalian mitotic exit as previously suggested in *Xenopus* (Mochida et al., 2009).

Recent data obtained in *Xenopus* suggest that PP2A may be inactivated by the Greatwall kinase (known as Mastl in mammals, a kinase that belongs to the AGC family represented by PKC, the original target of staurosporine), thus supporting the maintenance of Cdk-dependent phosphosites and the mitotic state (Castilho et al., 2009; Vigneron et al., 2009). Therefore, we tested whether the elimination of Mastl could cooperate in mitotic exit in Cdc20-deficient cells. Knockdown of Mastl by RNAi (siMastl) in *Cdc20*(Δ/Δ); *Pttg1*(Δ/Δ) double-mutant MEFs induces partial defects in mitotic entry (data not shown), consistent with a recent report in human cells (Burgess et al., 2010). However, most Cdc20 null cells eventually arrest in metaphase with high levels of phospho-Cdk substrates and without sister chromatid separation. Interestingly, *Cdc20*(Δ/Δ); *Pttg1*(Δ/Δ); Mastl RNAi cells quickly exit from mitosis after treatment with roscovitine. In these cells, Cdk substrates are dephosphorylated, and DNA decondenses generating tetraploid cells, in some cases containing micronuclei, most likely as a consequence of rapid decondensation without separation of sister chromatids (Figures 7D and 7E). Although this mitotic exit is abnormal because it is not accompanied by sister chromatid separation, we have utilized the term "mitotic exit" throughout the manuscript to indicate loss of mitotic properties (loss of rounded morphology, chromosome decondensation, loss of mitotic phospho-residues). The effect of RNAi against Mastl is specific because it can be rescued by transfecting Cdc20 null cells with a human Mastl cDNA insensitive to the RNAi oligonucleotides (Figure 7E). Thus, interference of Mastl expression synergizes with roscovitine in mitotic exit in Cdc20;securin-deficient cells. This cooperation is also observed in Cdc20 null cells in the presence of securin (data not shown), and it affects dephosphorylation of Cdk substrates, but not sister chromatid separation.

Mitotic Exit Requires Activation of PP2A/B55 Complexes

The combined effect of Mastl RNAi and roscovitine is suppressed by 500 nM OA, thus suggesting that PP2A acts downstream of Mastl during mammalian mitotic exit (Figure 7D). It has been recently proposed that B55δ is the regulatory subunit of PP2A in mitotic exit in *Xenopus* (Mochida et al., 2009). Indeed, whereas downregulation of all mammalian B55 genes (B55α,β,γ,δ) has no major effect on metaphase-arrested cells (Figure S6), it dramatically suppresses mitotic exit after combined inactivation of Cdk1 and Mastl (Figure 8A), suggesting that B55 proteins are the major regulatory subunits of PP2A during mitotic exit. The B55α (Ppp2r2a) and B55δ (Ppp2r2d) isoforms are widely expressed in mammalian cells (including fibroblasts), whereas B55β (Ppp2r2b) and B55γ (Ppp2r2c) are restricted to the nervous system (Eichhorn et al., 2009). In fact, downregulation of B55β does not prevent mitotic exit mediated by Cdk1 inhibition and Mastl suppression in Cdc20 null cells. However, suppression of B55α prevents 60% of mitotic exit (as determined by phosphorylation of Cdk substrates), whereas B55δ accounts for 40% of the phospho-Cdk-substrate signal (Figure 8B), indicating that both B55α and B55δ participate in the PP2A functional complexes required for mitotic exit in Cdc20 null fibroblasts. RNAi against B55 is also able to prevent mitotic exit in human or murine cells arrested with proteasome inhibitors (Figure S6). HeLa or B16F10 melanoma cells arrested in metaphase by MG132 do not exit from mitosis upon treatment with roscovitine, similar to other human cells (Potapova et al., 2006; Skoufias et al., 2007). However, concomitant treatment with roscovitine and Mastl RNAi results in rapid PP2A-B55-dependent mitotic exit (Figure S6).

Both PP1 and PP2A may participate in mitotic exit in *Xenopus* (Mochida et al., 2009; Wu et al., 2009). In this model, dephosphorylation of PP1 inhibitor-1 (Inh1) leads to its dissociation from the catalytic subunit and full PP1 activation (Wu et al., 2009). Therefore, we tested the effect of suppression of Inh1 in Cdc20 null cells. As shown in Figure S6, suppression of mouse Inh1 (Ppp1r1a) by RNAi results in a partial dephosphorylation of Cdk substrates in the presence of roscovitine. Interestingly, this exit is sensitive to 500 nM OA, suggesting that PP2A acts downstream of PP1 in mitotic exit. Thus, both phosphatases are likely to play a role in mammalian mitotic exit downstream of Cdc20, although their relative roles are yet to be established.

Altogether, these data suggest that the concomitant inhibition of Cdk1 and Mastl is a general mechanism for PP2A-mediated mitotic exit downstream of Cdc20 in both mouse and human cells. Whereas all Cdc20 null cells die in mitosis (Figure 6), a number of interphasic Cdc20 null cells in which Cdk1 and Mastl have been inhibited display increased viability and are able to enter into DNA replication (Figure S6). Thus, the inhibition of these mitotic kinases could counteract the therapeutic effect of inhibiting APC/C-Cdc20 in tumor cells.

DISCUSSION

Conditional genetic elimination of Cdc20 results in complete metaphase arrest in embryonic or somatic cells in vivo. Mitotic exit is likely to be efficient with as little as 5% of cellular Cdc20 (Wolthuis et al., 2008), giving an explanation for previous reports indicating that Cdc20 knockdown by RNAi does not result in cyclin B stabilization or mitotic arrest (Clarke, 2009). Cdh1 is not able to compensate for the lack of Cdc20. This is not due to differences in substrate specificity because Cdh1 is also able to target securin and cyclin B for degradation. Rather, this reflects the fact that Cdc20 absence arrests cells with high Cdk1 activity, and this activity is known to inhibit Cdh1 function (Manchado et al., 2010).

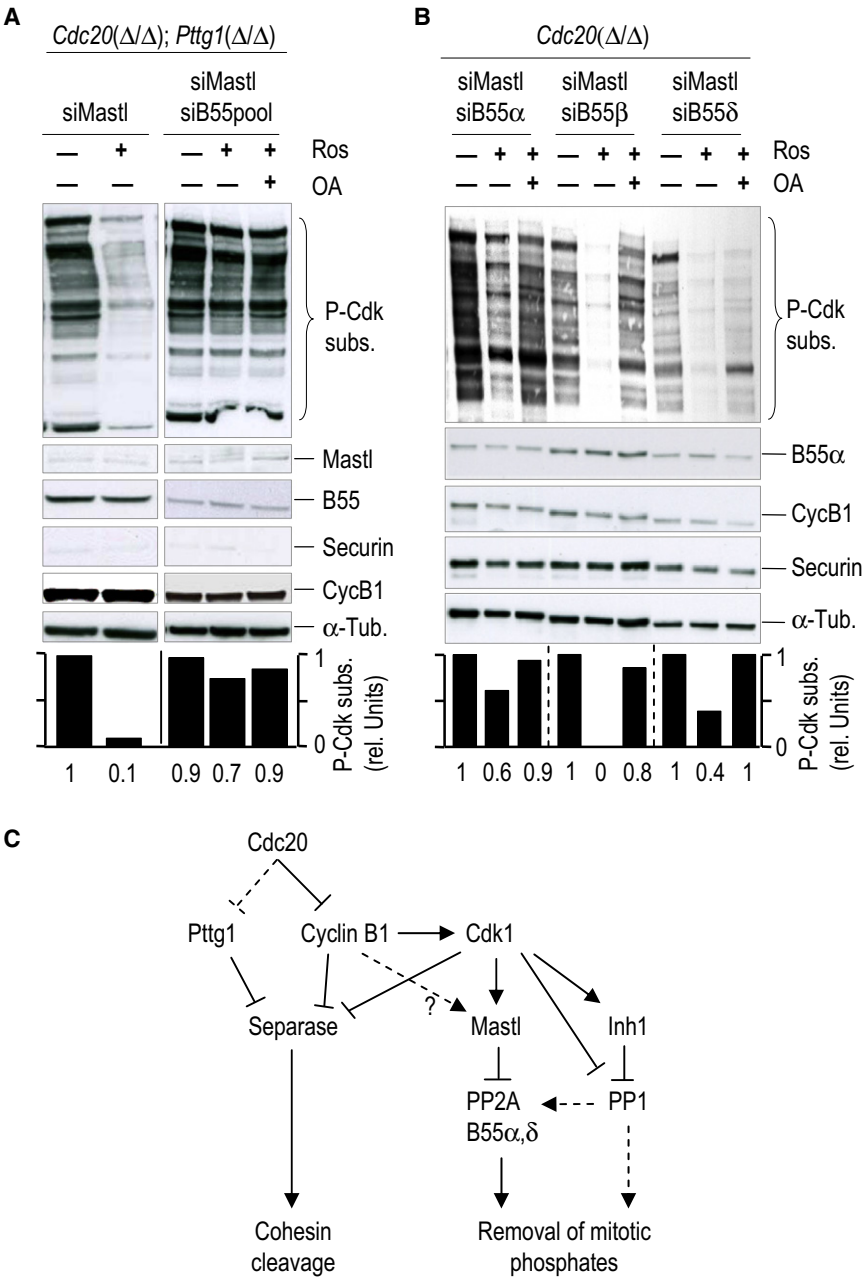

Figure 8. Mitotic Exit Is Inhibited by the Mastl Kinase and Requires PP2A-B55α,δ Complexes

(A) Double-mutant *Cdc20*(Δ/Δ); *Pttg1*(Δ/Δ) cells were transfected with specific siRNAs against Mastl (siMastl) and a pool of siRNAs against all B55 isoforms (siB55pool) showing that depletion of B55 prevents mitotic exit induced by siMastl + roscovitine (Ros), similar to treatment with okadaic acid (OA). The indicated proteins or phospho-epitopes are analyzed by immunoblotting, and the relative levels of phospho-Cdk-substrates are normalized versus control cultures without drugs. See Figure S6 for similar assays in human cells.

(B) Relative rescue of mitotic exit (as measured by the phospho-Cdk-substrate epitope) by specific siRNAs against B55α, B55β, and B55δ in Cdc20-deficient cells treated with roscovitine (Ros) and/or OA and siRNAs against Mastl (siMastl). The relative levels of phospho-Cdk-substrates or the indicated proteins are shown after immunoblot. Cdk-dependent phospho-residues are also quantified and normalized independently (relative to the respective control cells in the absence of Ros or OA that are arbitrarily set to "1") to eliminate relative differences in the loading of proteins.

(C) A model for mitotic exit induced by Cdc20 in mammals. The relevance of Pttg1/securin degradation by Cdc20 (dashed line) is not clear because it is dispensable in the presence of cyclin B, and Pttg1 levels are not significantly increased in Cdc20 null cells. Mastl is a critical node in the pathway to inactivate PP2A/B55α,δ complexes. The presence of cyclin B may inhibit mitotic exit, even upon chemical inhibition of Cdk1, e.g., by physical interaction with separase (Gorr et al., 2005) and perhaps Mastl (question mark).

Elimination of Cdc20 also has dramatic consequences for proliferation of tumor cells, in agreement with the recent proposal that targeting mitotic exit is a better cancer therapeutic strategy than targeting other cell cycle processes (Huang et al., 2009). Inhibiting mitotic exit is likely to also affect pRb null, p53 null, or SAC-deficient cells (Huang et al. [2009],and this work). The toxicity of Cdc20 ablation in proliferative cells is much stronger than any other treatment with available mitotic drugs, such as microtubule poisons (taxol or vincristine) or targeted inhibitors against Plk1 (BI2536) or the kinesin Eg5 (monastrol). Thus, the essential requirements for Cdc20 during mitosis suggest possible benefits of inhibiting APC/C function, e.g., by generating small molecules that prevent the APC/C-Cdc20 interaction. An interesting question that arises from these observations is whether Cdc20 null cells (or tumors cells treated with APC/C inhibitors) may adapt to this situation (exiting from mitosis without dying) and what the molecular requirements are for this exit.

We show here that Cdk1 and Mastl are required for Cdc20-dependent metaphase arrest and apoptosis. Inhibition of Cdk1 and Mastl strongly synergizes in mitotic exit in the absence of Cdc20 by generating tetraploid cells. Whether inhibition of Cdk1 alone by different small-molecule inhibitors is sufficient for mitotic exit in the presence of proteasome inhibitors is currently controversial, given the differences observed with different inhibitors (Potapova et al., 2009; Skoufias et al., 2007). At the concentrations used in this work, roscovitine is highly inefficient in inducing mitotic exit in the absence of Cdc20, although it induces a rapid exit from nocodazole arrest. Similarly, knockdown of Mastl alone is not sufficient for mitotic exit in Cdc20 null cells. However, inhibition of both kinases strongly synergizes and results in a dramatic removal of Cdk-dependent phosphates and rapid

PP2A-B55α,δ-dependent mitotic exit. These data suggest that partial Cdk1 inhibition is likely to be insufficient to drive mitotic exit because Cdk1 substrates are already phosphorylated, and they cannot be dephosphorylated as long as Mastl remains active.

Activation of Cdc20 should lead to the inactivation of both Cdk1 and Mastl, resulting in PP2A activation (Figure 8C). How Mastl is inactivated downstream of Cdc20 is not clear at this moment. Mastl contains a consensus KEN box and several putative D-box domains, although we have not been able to demonstrate APC/C-mediated degradation of this kinase (Figure S6). One possibility is that in Cdc20 null cells direct interaction between cyclin B1 and Mastl (Figure 8C) prevents the efficient inactivation of this protein, even upon chemical inhibition of Cdk1. This is not a novel mechanism because direct interaction between cyclin B1 and separase inhibits this protease, even if Cdk1-dependent phospho-residues have been eliminated (Boos et al., 2008; Gorr et al., 2005). We have also observed co-immunoprecipitation of Mastl and cyclin B1 in the same protein complexes (data not shown). Because Mastl has been proposed to be modulated by Cdk1-dependent phosphorylation (Yu et al., 2006), it is difficult to discriminate whether this represents normal phosphorylation of Mastl by cyclin B1-Cdk1 complexes or a phosphorylation-independent interaction. The fact that roscovitine is insufficient for dephosphorylation of Cdk substrates, and this is rescued by Mastl knockdown, suggests that Mastl or the putative Mastl substrates need to be dephosphorylated prior to the activation of PP2A. Suppression of the PP1 inhibitor Inh1 results in a partial exit from mitosis in the presence of roscovitine, thus suggesting that PP1 could also participate in this pathway as previously proposed in *Xenopus* (Wu et al., 2009) (Figure 8C). For instance, PP1 may be responsible for the elimination of activating phosphates on Mastl or the removal of Mastl-dependent phosphates in its substrates (Castilho et al., 2009). In agreement with this proposal, PP1 is likely to act upstream of PP2A because the effect of Inh1 suppression is sensitive to OA. Further focused work will be necessary to compare the relative roles of these two phosphatases during mitotic exit in mammals. In Cdc20 null cells the elimination of Mastl is necessary to activate PP2A, and full mitotic exit requires both PP2A/B55α and PP2A/B55δ complexes. Because B55β and B55γ are not expressed in primary MEFs, these results are likely to represent the relative amount of each of these isoforms in a particular cell type.

Altogether, these results indicate that Cdc20 is an essential driver of mitotic exit in mammalian normal or tumor cells and that mitotic exit requires Mastl inhibition and the activation of PP2A-B55α,δ phosphatases. Upon elimination of Cdc20, tumor cells rapidly die of apoptosis in vitro and in vivo unless Cdk1 and Mastl kinases are inhibited. This molecular pathway may have relevant implications for designing future therapeutic strategies aimed at inhibiting APC/C and for preventing adaptation to the apoptotic cell death imposed by defective mitotic exit. How to use these strategies and how to discriminate between normal and tumor cells have been recently reviewed (Gascoigne and Taylor, 2009; Rieder and Medema, 2009). For instance, chemical APC/C-Cdc20 inhibitors could be used as a combinatory therapy with other mitotic poisons. Partial Cdc20 inhibition may delay mitotic exit, preventing slippage of tumoral cells, which is one of the most important mechanisms of resistance in tumor treated with mitotic drugs. Other strategies to consider may be the protection of normal cells by impeding their entry into the cell cycle. For instance, prolonged fasting concomitant to the delivery of chemotherapy dramatically reduces the toxic side effects of the treatment, while maintaining its efficacy against cancer (Raffaghello et al., 2008). Other studies suggest the use of G1 inhibitors (e.g., Cdk4/2 inhibitors) to arrest normal cells (pRb proficient) in G0/G1, thus protecting them from toxic chemotherapies. pRb null tumor cells that do not respond to these chemicals would enter into the cell cycle, thereby making them sensitive to chemotoxic treatments (Blagosklonny and Pardee, 2001). Thus, on one hand, partial Cdc20 inhibition may synergize with microtubule poisons, but combination with Cdk1 inhibitors should be avoided. On the other hand, strong inhibition of APC/C-Cdc20 is likely to be highly efficient in inducing apoptotic cell death, and this property should be used in therapeutic scenarios in which proliferation of normal cells is abrogated, such as after food starvation or in combination with G1-arresting agents, to selectively protect these normal cells against efficient mitotic chemotherapies.

EXPERIMENTAL PROCEDURES

Generation and Characterization of Cdc20 Mutant Mice

The *Cdc20* exon 2 was flanked with loxP sites as indicated in Figure S1. The conditions for genotyping Cdc20 mutant are available from the authors upon request. Securin conditional mutants and RERT2 mice were genotyped as described (Guerra et al., 2003; Wirth et al., 2006). Mouse depilation (Ruzankina et al., 2007) and induction of skin tumors (Sotillo et al., 2001b) were performed as reported previously. Mutant mice were fed with 4-OHT-supplemented food (Harlan Laboratories Models), injected (i.p.) as described by Perera et al. (2007), or topically painted with 50 μl 4-OHT (5 mg/ml). All animals were maintained in a mixed 129/Sv (25%) × CD1 (25%) × C57BL/6J (50%) background. Xenographs were generated using transformed MEFs using SCID mice (Charles Rivers) essentially as described previously (Sotillo et al., 2001a). These mice were treated with taxol (Paclitaxel, Sigma; 12 mg/kg), vincristine (Sigma; 12 mg/kg), and BI2536 (Selleck Chemicals; 35 mg/kg) following the recommended doses reported previously (Koyanagi et al., 1994; Patel et al., 2010; Steegmaier et al., 2007). All animal protocols were approved by the ISCIII committee for animal care and research. For histological observation, dissected organs were fixed in 10% buffered formalin (Sigma) and embedded in paraffin wax. Sections of 3 or 5 μm thickness were stained with hematoxylin and eosin (H&E). Immunohistochemistry was performed using specific antibodies against the following antigens: BrdU (GE Healthcare), Ki67 (Dako), active caspase 3 (Cell Signaling Technology), cyclin B1 (Chemical International), Cdc20 (Santa Cruz Biotechnology), and CD34 (Abcam).

Cell Culture and Treatments

MEFs were isolated from E13.5 embryos and cultured essentially as described previously (Garcia-Higuera et al., 2008). Adenoviruses expressing GFP or Cre (supplied by the Iowa University) and siRNAs against specific transcripts (Dharmacon) were used following the manufacturer's recommendations. Briefly, adenoviruses were transduced in confluency, and cells were split 48 hr after and transfected with siRNAs when required. The following drugs were used in cultured cells at the indicated concentrations: nocodazole (Sigma; 100 ng/ml); roscovitine (Sigma; 1–200 μM; see figure legends); purvalanol A (Calbiochem; 10–100 μM); RO-3306 (Calbiochem; 10–100 μM); GCP-74514A (Calbiochem; 10–100 μM); Staurosporine (Sigma; 0.1, 1, and 10 μM); Plk1 inhibitors GW843682X (Tocris; 10–100 μM) and BI2536 (Selleck Chemicals; 100 nM); Aurora B inhibitor ZM447439 (Tocris; 10–100 μM); taxol (Sigma; 200 nM); and vincristine (Sigma; 1 μM) and monastrol (Sigma; 100 μM). The concentration of taxol, vincristine, BI2536, and monastrol was selected after testing the minimum saturating concentration required to induce mitotic arrest in MEFs. MEFs were transformed with H-ras and E1A oncogenes

essentially as reported previously (Quereda et al., 2007), and xenographs were generated by subcutaneous injection of 5×10^5 cells in SCID mice. For videomicroscopy, H2B-GFP expressing cells were recorded using a Deltavision Apparatus (Applied Precision) using 10 min frames during 72 hr.

Metaphase Spreads

Cells were hypotonically swollen in 40% full medium/60% tap water for 5.5 min. Hipotonic treatment is stopped by adding an equal volume of Carnoy's solution (75% pure methanol, 25% glacial acetic acid), cells are then spun down and resuspended and fixed with Carnoy's solution for 10 min. After fixation cells are dropped from a 5 cm height onto glass slides. Slides are stained with 5% Giemsa in PBS for 7 min.

Immunofluorescence and Biochemical Analysis

Embryos were fixed with cold methanol during 1 hr at −20°C, rinsed with M2 medium, washed in PBS containing 0.1% BSA (Sigma), and incubated with 0.1% Triton X for permeabilization. Embryos were then blocked with 3% BSA and incubated with primary antibodies (see below) for 2–4 hr at 37°C. The matching secondary antibodies (Alexa 488, 594, or 647) are from Molecular Probes (Invitrogen). Images were obtained using a confocal ultra-spectral microscope (Leica TCS-SP5-AOBS-UV). Cultured cells were grown in coverslips, fixed with 4% paraformaldehyde in PBS for 7 min at 37°C, permeabilized with PBS-Triton 0.15% for 2 min at 37°C, and blocked with 1% BSA for 1 hr. Immunofluorescence in embryos or cultured cells was performed using specific antibodies against the following proteins: phospho-histone H3 (Millipore), α-tubulin (Sigma), and ACA (Antibodies Incorporated). For Western blotting, cells were harvested and lysed in RIPA buffer, and 50 μg of total protein was separated by SDS-PAGE and probed with antibodies against securin (Abcam), Cdc20 (Santa Cruz), phosphoSer-CDKs substrates (Cell Signaling Technology), cyclin B1 (Chemicon International), MASTL (Abcam), Inhibitor 1 (Ppp1r1a) (Abcam), B55 (Santa Cruz), alpha-tubulin (Sigma), phospho-Histone 3 (Millipore), cyclin A2 (Santa Cruz), Mad2 (MBL), $p21^{Cip1}$ (Santa Cruz), and α-Actin and α-tubulin (Sigma).

Statistical Analysis

Statistical analysis was performed using Student's t, chi-square, or log-rank tests (GraphPad Prism 5). All data are shown as mean ± SD; probabilities of $p < 0.05$ were considered significant.

SUPPLEMENTAL INFORMATION

Supplemental Information includes Supplemental Experimental Procedures and six figures and can be found with this article online at doi:10.1016/j.ccr.2010.10.028.

ACKNOWLEDGMENTS

We are indebted to Gardenia Fresneda for generation of the Cdc20-targeting vector and members of the Comparative Pathology, Molecular Imaging and Transgenic Mice facilities of the CNIO for their excellent technical support. We thank K. Nasmyth for sharing securin-mutant mice. E.M., M.G., and M.E are supported by fellowships from the Ministerio de Ciencia e Innovación (MICINN). M.T. and H.Y. are supported by Marie Curie Cancer Care and the Association for International Cancer Research (AICR). M.M. and S.M. wish to acknowledge the Fundación Científica de la Asociación Española contra el Cáncer for financial support. I.G.-H. and S.M. are supported by grants BFU2008-01808, Consolider CSD2007-00015, and Junta de Castilla y León Grupo de Excelencia GR 265. The Cell Division and Cancer group of the CNIO is funded by the MICINN (SAF2009-07973), Consolider-Ingenio 2010 Programme (CSD2007-00017), Comunidad de Madrid (OncoCycle Programme; S-BIO-0283-2006), Fundación Ramón Areces, AICR (08-0188), and the MitoSys project (HEALTH-F5-2010-241548; European Union Seventh Framework Program).

Received: May 2, 2010
Revised: August 13, 2010
Accepted: October 13, 2010
Published: December 13, 2010

REFERENCES

Bain, J., Plater, L., Elliott, M., Shpiro, N., Hastie, C.J., McLauchlan, H., Klevernic, I., Arthur, J.S., Alessi, D.R., and Cohen, P. (2007). The selectivity of protein kinase inhibitors: a further update. Biochem. J. *408*, 297–315.

Baumgarten, A.J., Felthaus, J., and Wäsch, R. (2009). Strong inducible knockdown of APC/CCdc20 does not cause mitotic arrest in human somatic cells. Cell Cycle *8*, 643–646.

Blagosklonny, M.V., and Pardee, A.B. (2001). Exploiting cancer cell cycling for selective protection of normal cells. Cancer Res. *61*, 4301–4305.

Boos, D., Kuffer, C., Lenobel, R., Korner, R., and Stemmann, O. (2008). Phosphorylation-dependent binding of cyclin B1 to a Cdc6-like domain of human separase. J. Biol. Chem. *283*, 816–823.

Burgess, A., Vigneron, S., Brioudes, E., Labbe, J.C., Lorca, T., and Castro, A. (2010). Loss of human Greatwall results in G2 arrest and multiple mitotic defects due to deregulation of the cyclin B-Cdc2/PP2A balance. Proc. Natl. Acad. Sci. USA *107*, 12564–12569.

Castilho, P.V., Williams, B.C., Mochida, S., Zhao, Y., and Goldberg, M.L. (2009). The M phase kinase Greatwall (Gwl) promotes inactivation of PP2A/B55delta, a phosphatase directed against CDK phosphosites. Mol. Biol. Cell. *20*, 4777–4789.

Clarke, D.J. (2009). Strong inducible knockdown of Cdc20 does not cause mitotic arrest in human somatic cells: implications for cancer therapy? Cell Cycle *8*, 515–516.

D'Angiolella, V., Mari, C., Nocera, D., Rametti, L., and Grieco, D. (2003). The spindle checkpoint requires cyclin-dependent kinase activity. Genes Dev. *17*, 2520–2525.

Eichhorn, P.J., Creyghton, M.P., and Bernards, R. (2009). Protein phosphatase 2A regulatory subunits and cancer. Biochim. Biophys. Acta *1795*, 1–15.

Felix, M.A., Cohen, P., and Karsenti, E. (1990). Cdc2 H1 kinase is negatively regulated by a type 2A phosphatase in the Xenopus early embryonic cell cycle: evidence from the effects of okadaic acid. EMBO J. *9*, 675–683.

Garcia-Higuera, I., Manchado, E., Dubus, P., Canamero, M., Mendez, J., Moreno, S., and Malumbres, M. (2008). Genomic stability and tumour suppression by the APC/C cofactor Cdh1. Nat. Cell Biol. *10*, 802–811.

Gascoigne, K.E., and Taylor, S.S. (2008). Cancer cells display profound intra- and interline variation following prolonged exposure to antimitotic drugs. Cancer Cell *14*, 111–122.

Gascoigne, K.E., and Taylor, S.S. (2009). How do anti-mitotic drugs kill cancer cells? J. Cell Sci. *122*, 2579–2585.

Gimenez-Abian, J.F., Diaz-Martinez, L.A., Wirth, K.G., De la Torre, C., and Clarke, D.J. (2005). Proteasome activity is required for centromere separation independently of securin degradation in human cells. Cell Cycle *4*, 1558–1560.

Gorr, I.H., Boos, D., and Stemmann, O. (2005). Mutual inhibition of separase and Cdk1 by two-step complex formation. Mol. Cell *19*, 135–141.

Guerra, C., Mijimolle, N., Dhawahir, A., Dubus, P., Barradas, M., Serrano, M., Campuzano, V., and Barbacid, M. (2003). Tumor induction by an endogenous K-ras oncogene is highly dependent on cellular context. Cancer Cell *4*, 111–120.

Huang, H.C., Shi, J., Orth, J.D., and Mitchison, T.J. (2009). Evidence that mitotic exit is a better cancer therapeutic target than spindle assembly. Cancer Cell *16*, 347–358.

Jackson, S.P., and Bartek, J. (2009). The DNA-damage response in human biology and disease. Nature *461*, 1071–1078.

Jordan, M.A., and Wilson, L. (2004). Microtubules as a target for anticancer drugs. Nat. Rev. Cancer *4*, 253–265.

Kavallaris, M. (2010). Microtubules and resistance to tubulin-binding agents. Nat. Rev. Cancer *10*, 194–204.

Koyanagi, N., Nagasu, T., Fujita, F., Watanabe, T., Tsukahara, K., Funahashi, Y., Fujita, M., Taguchi, T., Yoshino, H., and Kitoh, K. (1994). In vivo tumor growth inhibition produced by a novel sulfonamide, E7010, against rodent and human tumors. Cancer Res. *54*, 1702–1706.

Li, M., York, J.P., and Zhang, P. (2007). Loss of Cdc20 causes a securin-dependent metaphase arrest in two-cell mouse embryos. Mol. Cell. Biol. *27*, 3481–3488.

Malumbres, M., and Barbacid, M. (2001). To cycle or not to cycle: a critical decision in cancer. Nat. Rev. Cancer *1*, 222–231.

Malumbres, M., and Barbacid, M. (2007). Cell cycle kinases in cancer. Curr. Opin. Genet. Dev. *17*, 60–65.

Malumbres, M., and Barbacid, M. (2009). Cell cycle, CDKs and cancer: a changing paradigm. Nat. Rev. Cancer *9*, 153–166.

Manchado, E., Eguren, M., and Malumbres, M. (2010). The anaphase-promoting complex/cyclosome (APC/C): cell-cycle-dependent and -independent functions. Biochem. Soc. Trans. *38*, 65–71.

Mochida, S., Ikeo, S., Gannon, J., and Hunt, T. (2009). Regulated activity of PP2A-B55 delta is crucial for controlling entry into and exit from mitosis in Xenopus egg extracts. EMBO J. *28*, 2777–2785.

Patel, N., Chatterjee, S.K., Vrbanac, V., Chung, I., Mu, C.J., Olsen, R.R., Waghorne, C., and Zetter, B.R. (2010). Rescue of paclitaxel sensitivity by repression of Prohibitin1 in drug-resistant cancer cells. Proc. Natl. Acad. Sci. USA *107*, 2503–2508.

Perera, D., Tilston, V., Hopwood, J.A., Barchi, M., Boot-Handford, R.P., and Taylor, S.S. (2007). Bub1 maintains centromeric cohesion by activation of the spindle checkpoint. Dev. Cell *13*, 566–579.

Peters, J.M. (2006). The anaphase promoting complex/cyclosome: a machine designed to destroy. Nat. Rev. Mol. Cell Biol. *7*, 644–656.

Potapova, T.A., Daum, J.R., Pittman, B.D., Hudson, J.R., Jones, T.N., Satinover, D.L., Stukenberg, P.T., and Gorbsky, G.J. (2006). The reversibility of mitotic exit in vertebrate cells. Nature *440*, 954–958.

Potapova, T.A., Daum, J.R., Byrd, K.S., and Gorbsky, G.J. (2009). Fine tuning the cell cycle: activation of the Cdk1 inhibitory phosphorylation pathway during mitotic exit. Mol. Biol. Cell *20*, 1737–1748.

Queralt, E., and Uhlmann, F. (2008). Cdk-counteracting phosphatases unlock mitotic exit. Curr. Opin. Cell Biol. *20*, 661–668.

Quereda, V., Martinalbo, J., Dubus, P., Carnero, A., and Malumbres, M. (2007). Genetic cooperation between p21Cip1 and INK4 inhibitors in cellular senescence and tumor suppression. Oncogene *26*, 7665–7674.

Raffaghello, L., Lee, C., Safdie, F.M., Wei, M., Madia, F., Bianchi, G., and Longo, V.D. (2008). Starvation-dependent differential stress resistance protects normal but not cancer cells against high-dose chemotherapy. Proc. Natl. Acad. Sci. USA *105*, 8215–8220.

Rieder, C.L., and Medema, R.H. (2009). No way out for tumor cells. Cancer Cell *16*, 274–275.

Ruzankina, Y., Pinzon-Guzman, C., Asare, A., Ong, T., Pontano, L., Cotsarelis, G., Zediak, V.P., Velez, M., Bhandoola, A., and Brown, E.J. (2007). Deletion of the developmentally essential gene ATR in adult mice leads to age-related phenotypes and stem cell loss. Cell Stem Cell *1*, 113–126.

Shirayama, M., Toth, A., Galova, M., and Nasmyth, K. (1999). APC(Cdc20) promotes exit from mitosis by destroying the anaphase inhibitor Pds1 and cyclin Clb5. Nature *402*, 203–207.

Skoufias, D.A., Indorato, R.L., Lacroix, F., Panopoulos, A., and Margolis, R.L. (2007). Mitosis persists in the absence of Cdk1 activity when proteolysis or protein phosphatase activity is suppressed. J. Cell Biol. *179*, 671–685.

Sotillo, R., Dubus, P., Martin, J., de la Cueva, E., Ortega, S., Malumbres, M., and Barbacid, M. (2001a). Wide spectrum of tumors in knock-in mice carrying a Cdk4 protein insensitive to INK4 inhibitors. EMBO J. *20*, 6637–6647.

Sotillo, R., Garcia, J.F., Ortega, S., Martin, J., Dubus, P., Barbacid, M., and Malumbres, M. (2001b). Invasive melanoma in Cdk4-targeted mice. Proc. Natl. Acad. Sci. USA *98*, 13312–13317.

Steegmaier, M., Hoffmann, M., Baum, A., Lénárt, P., Petronczki, M., Krssák, M., Gürtler, U., Garin-Chesa, P., Lieb, S., Quant, J., et al. (2007). BI 2536, a potent and selective inhibitor of polo-like kinase 1, inhibits tumor growth in vivo. Curr. Biol. *17*, 316–322.

Stegmeier, F., and Amon, A. (2004). Closing mitosis: the functions of the Cdc14 phosphatase and its regulation. Annu. Rev. Genet. *38*, 203–232.

Sullivan, M., and Morgan, D.O. (2007). Finishing mitosis, one step at a time. Nat. Rev. Mol. Cell Biol. *8*, 894–903.

Syljuasen, R.G. (2007). Checkpoint adaptation in human cells. Oncogene *26*, 5833–5839.

Thornton, B.R., and Toczyski, D.P. (2003). Securin and B-cyclin/CDK are the only essential targets of the APC. Nat. Cell Biol. *5*, 1090–1094.

Vigneron, S., Brioudes, E., Burgess, A., Labbe, J.C., Lorca, T., and Castro, A. (2009). Greatwall maintains mitosis through regulation of PP2A. EMBO J. *28*, 2786–2793.

Wäsch, R., and Cross, F.R. (2002). APC-dependent proteolysis of the mitotic cyclin Clb2 is essential for mitotic exit. Nature *418*, 556–562.

Weaver, B.A., and Cleveland, D.W. (2005). Decoding the links between mitosis, cancer, and chemotherapy: The mitotic checkpoint, adaptation, and cell death. Cancer Cell *8*, 7–12.

Wirth, K.G., Wutz, G., Kudo, N.R., Desdouets, C., Zetterberg, A., Taghybeeglu, S., Seznec, J., Ducos, G.M., Ricci, R., Firnberg, N., et al. (2006). Separase: a universal trigger for sister chromatid disjunction but not chromosome cycle progression. J. Cell Biol. *172*, 847–860.

Wolthuis, R., Clay-Farrace, L., van Zon, W., Yekezare, M., Koop, L., Ogink, J., Medema, R., and Pines, J. (2008). Cdc20 and Cks direct the spindle checkpoint-independent destruction of cyclin A. Mol. Cell *30*, 290–302.

Wu, J.Q., Guo, J.Y., Tang, W., Yang, C.S., Freel, C.D., Chen, C., Nairn, A.C., and Kornbluth, S. (2009). PP1-mediated dephosphorylation of phosphoproteins at mitotic exit is controlled by inhibitor-1 and PP1 phosphorylation. Nat. Cell Biol. *11*, 644–651.

Yu, J., Zhao, Y., Li, Z., Galas, S., and Goldberg, M.L. (2006). Greatwall kinase participates in the Cdc2 autoregulatory loop in Xenopus egg extracts. Mol. Cell *22*, 83–91.